An Analytical Model for $I-V$ and Small-Signal Characteristics of Planar-Doped HEMT's

GUAN-WU WANG AND LESTER F. EASTMAN, FELLOW, IEEE

Abstract—An analytical current–voltage model for planar-doped HEMT's has been developed. This compact model is able to cover the complete HEMT $I-V$ characteristics, including the current saturation region and the parasitic conduction in the electron-supplying layer. Analytical expressions of small-signal parameters and current gain cutoff frequency (f_T) are derived from the $I-V$ model. Modeling results of a 0.1-μm-gate planar-doped AlInAs/GaInAs HEMT show excellent agreement with measured characteristics. Threshold voltages and parasitic conduction in planar-doped and uniformly doped HEMT's are also compared and discussed.

I. Introduction

THE FIRST AlGaAs/GaAs high electron mobility transistor (HEMT) model for channel charge and current as functions of gate and drain voltages was developed by Delagebeaudeuf and Lihn [1]. Lee *et al.* extended this model to include the variation of Fermi energy of the two-dimensional electron gas (2DEG) with carrier density [2], [3]. The parasitic conduction in the AlGaAs layer at high gate voltage was discussed in [4]. However, the piecewise velocity-field relation used in Lee's model leads to piecewise current–voltage characteristics. The $I-V$ characteristics after current saturation were not modeled either. The computer-aided design and simulation of HEMT circuits demand a more accurate and complete model. A compact and complete model which is able to cover the whole current–voltage characteristic, including the transconductance compression effect, is given in [5]. This analytical model has been applied to time-domain large-signal simulation of HEMT circuits [6]. The simulation results indicate that transconductance compression plays a significant role in the large-signal simulation.

Recently, the planar doping technique has found wide applications in various HEMT structures in different material systems [7], [8]. This doping technique utilizes a silicon donor plane as the electron supplier, which is deposited during MBE growth by growth interrupt. This technique is attractive because of its lower doping compensation rate and higher 2DEG density [9], good device breakdown characteristics [10], and reduced concentration of DX center in the AlGaAs layer [11]. However, presently available HEMT models as discussed above are all developed for the uniformly doped HEMT's. Since the electron states of silicon donors in the planar-doped heterostructure also show two-dimensional characteristics [12], similar to the 2DEG accumulated at the heterointerface, the charge control of planar-doped HEMT's is therefore different from that of uniformly doped HEMT's. In this work, a current–voltage and small-signal model for planar-doped HEMT's is developed by extending our previous uniformly doped HEMT $I-V$ model [5]. The new model also provides a physical basis for predicting the microwave performance.

Manuscript received December 12, 1988; revised April 14, 1989.

G.-W. Wang was with the School of Electrical Engineering, Cornell University, Ithaca, NY 14853. He is now with Ford Microelectronics, Inc., 10340 State Highway 83 N, Colorado Springs, CO 80921.

L. F. Eastman is with the School of Electrical Engineering, Cornell University, Ithaca, NY 14853.

IEEE Log Number 8928997.

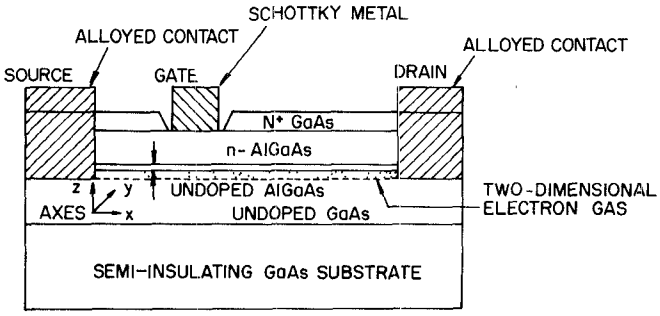

Fig. 1. Schematic diagram of a typical AlGaAs/GaAs HEMT.

II. Uniform Doping and Planar Doping

The most significant difference between uniformly doped and planar-doped HEMT's lies in the charge control of the parasitic conduction. A schematic diagram of the typical AlGaAs/GaAs HEMT, which is a HEMT in its simplest form, is shown in Fig. 1. There are two current conducting paths: one through the 2DEG channel and the other through the undepleted AlGaAs region. Under normal bias conditions, the AlGaAs layer under the gate is fully depleted by the Schottky gate and the AlGaAs/GaAs heterointerface. As the gate voltage increases above a certain turn-on voltage, parasitic electrons start to be induced in the undepleted AlGaAs region. In a uniformly doped AlGaAs layer, the charge control of these parasitic electrons will behave similarly to that of a MESFET [4]. In contrast, the charge control of the planar-doped AlGaAs layer assumes a linear form similar to that of a 2DEG. The exact form of the charge control of these parasitic electrons will be given in the next section.

0018-9480/89/0900-1395$01.00

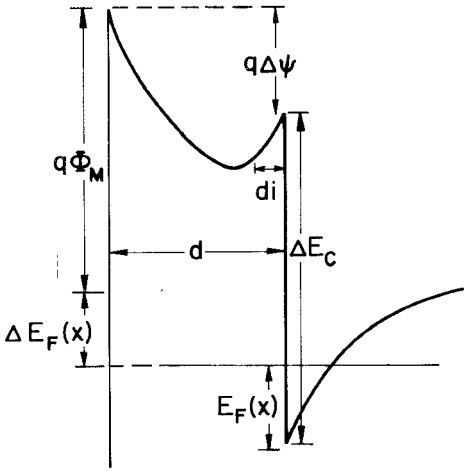

Fig 2 Conduction band diagram of a uniformly doped HEMT.

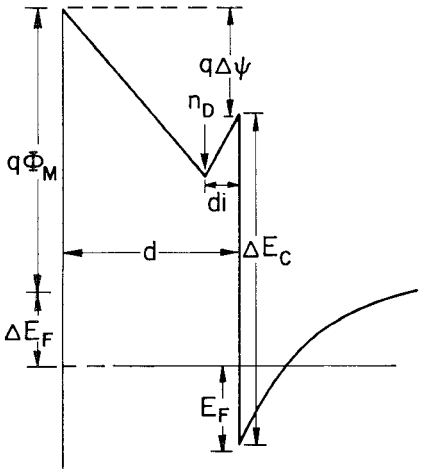

Fig. 3. Conduction band diagram of a planar-doped HEMT

Since the potential distribution due to ionized donors is different in the two types of HEMT's, the corresponding threshold voltage of the 2DEG also varies. The threshold voltage of a uniformly doped HEMT can be easily derived. Assuming all the silicon donors are ionized and the electrons are transferred to the 2DEG, with the aid of Fig. 2, Poisson's equation can be solved to obtain the threshold voltage [2]:

$$V_{\text{th}} = \Phi_M + \frac{E_{F0}}{q} - \frac{qN_d}{2\epsilon_2}(d - d_i)^2 - \frac{\Delta E_c}{q} \tag{1}$$

where a linear relationship between Fermi level and 2DEG charge density is assumed [2], i.e.,

$$E_F = an_s + E_{F0} \tag{2}$$

in which E_{F0} is the Fermi level at zero 2DEG density and a is a constant depending on the material properties. A list of the symbols used is given in Appendix I.

The conduction band diagram of a planar-doped heterostructure is shown in Fig. 3. The electron states in the V-shaped quantum well in the electron-supplying layer, e.g., the AlGaAs layer in AlGaAs/GaAs HEMT's, are also quantized in the same way as the 2DEG channel at the heterointerface [12]. Solving Poisson's equation with Fig. 3 yields

$$\Delta E_F = q\Phi_M + E_F - \Delta E_c + \frac{q^2 dn_s}{\epsilon_2} + \frac{q^2 n_2^*(d - d_i)}{\epsilon_2} - \frac{q^2 n_D(d - d_i)}{\epsilon_2} \tag{3}$$

where n_s^* is the sheet density of the electrons in the V-shaped quantum well, and n_D is the sheet density of the silicon doping plane. ΔE_F arises from the nonequilibrium situation due to the external gate and drain biases to the device, and $\Delta E_F = -qV_G$ at zero drain voltage. Before parasitic conduction in the electron-supplying layer starts, $n_s^* = 0$ and one obtains the threshold voltage of the planar-doped HEMT by rearranging (3):

$$V_{\text{th}} = \Phi_M + \frac{E_{F0}}{q} - \frac{qn_D(d - d_i)}{\epsilon_2} - \frac{\Delta E_c}{q}. \tag{4}$$

According to (4), the threshold voltage of a planar-doped HEMT is a linear function of the thickness of the electron-supplying layer, while a quadratic relationship for the uniformly doped HEMT is shown in (1). As a result of the linear dependence, the characteristics of the circuits and devices fabricated on the planar-doped structures will show more uniformity and be less sensitive to the growth and processing variations.

III. Current–Voltage Model

The current–voltage equations derived for uniformly doped AlGaAs/GaAs HEMT's [5] are included in Appendix II. A list of the symbols used in these equations is given in Appendix I. Note that the validity of this model is not limited to the AlGaAs/GaAs material system. By changing the corresponding material parameters, this model can be applied to uniformly doped HEMT's in other material systems such as AlInAs/GaInAs heterostructures. To be equally useful for planar-doped HEMT's, these equations require slight modifications. Since the charge control of the 2DEG has the same linear form for these two types of HEMT's, except that the threshold voltages are different, the equations for the 2DEG channel current in Appendix II are directly applicable to planar-doped HEMT's. The major difference comes from the charge control of the parasitic electrons in the electron-supplying layer. Consequently, the expressions for parasitic conduction currents have to be modified.

When the electrons in the 2DEG channel reach equilibrium concentration, which is also the maximum number of electrons the 2DEG channel can accommodate, the gate begins to induce electrons in the V-shaped quantum well. Combining (3) and (4), the charge control of sheet electron density in the V-shaped quantum well by gate voltage and channel potential under the gate is given by

$$n_s^* = \frac{C_0^*}{q}(V_G - V_{\text{th}}^* - V) \tag{5}$$

where

$$C_0^* = \frac{q\epsilon_2}{d-d_i} \tag{6}$$

$$V_{\text{th}}^* = \Phi_M + \frac{an_{s0}}{q} + \frac{E_{F0}}{q} - \frac{qn_D(d-d_i)}{\epsilon_2} + \frac{qdn_{s0}}{\epsilon_2} - \frac{\Delta E_c}{q} \tag{7}$$

in which n_{s0} is the equilibrium sheet density of the 2DEG. Note that this charge control of the parasitic conduction has the same form as that of the 2DEG [2], [5].

Following the same analysis as in [5], one obtains the parasitic conduction current. When $V_D \leq V_G - V_{\text{th}}^*$,

$$I_1 = \frac{E^*}{1+\frac{V_D}{F}}\left[(V_G - V_{\text{th}}^*)V_D - \frac{V_D^2}{2}\right] \tag{8}$$

where

$$E^* = \frac{Z\mu_1 C_0^*}{L} \tag{9}$$

and when $V_D > V_G - V_{\text{th}}^*$,

$$I_1 = \frac{E^*(V_G - V_{\text{th}}^*)}{2\left[\frac{A(V_{\text{th}}^* - V_{\text{th}})}{I_2} - \frac{1}{B} + \frac{1}{F}\right]}. \tag{10}$$

With equations (A9), (A10), and (A14) replaced by (8), (9), and (10), and V_c by V_{th}^*, the original set of $I-V$ equations in Appendix II is adapted to planar-doped HEMT's. Equations (A8) and (A13) represent the 2DEG current in the active channel and remain unchanged.

The $I-V$ equations for planar-doped HEMT's are used to model the 0.1-μm-gate AlInAs/GaInAs HEMT on GaAs substrate [8]. This device shows a peak extrinsic dc transconductance of 585 mS/mm and a full channel current of 370 mA/mm. Close agreement between the measured and modeled $I-V$ characteristics is shown in Fig. 4, which we found could not be achieved by using the original $I-V$ equations in Appendix II.

In spite of the extremely short gate length, the $I-V$ equations for the planar-doped HEMT still give an excellent modeling. The measured $I-V$ characteristic shows the kink effect [13], which is not included in the model. Since the kink effect appears only in AlInAs/GaInAs material system, these $I-V$ equations are still suitable for general application of planar-doped HEMT modeling. In this example, a 3.2 kΩ parallel resistance from drain to source is included in the modeling to account for the substrate leakage current [8]. A global fitting program is used to determine the modeling parameters [5]. The modeling parameters A, B, E, and F are directly related to the material properties and the device feature sizes. The initial values of these parameters can then be estimated using the published material data. The modeling parameters for a best fit are found to be $V_{\text{th}} = -0.33$ V, $V_{\text{th}}^* = -0.15$ V, $A = 67.62$ mA/V^2, $B = 0.146$ V, $C = 5.4$ Ω, $E = 15.08$ mA/V^2, and $F = 0.197$ V.

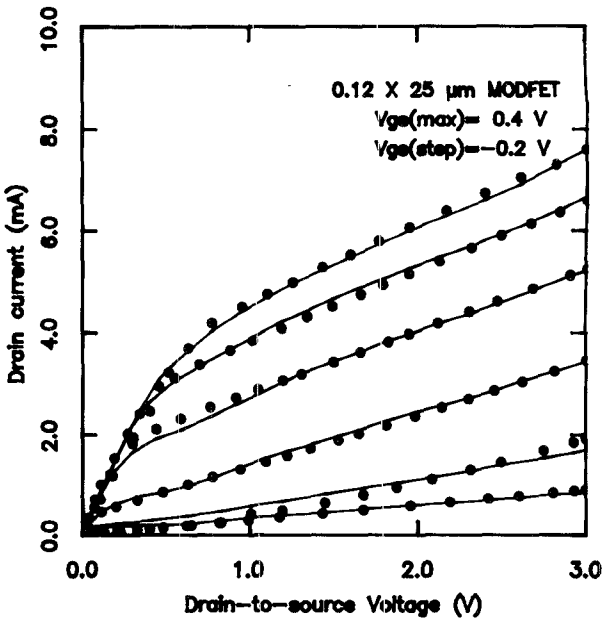

Fig. 4. Measured and modeled $I-V$ characteristics of the 0.12×50 μm AlInAs/GaInAs HEMT. Solid line: measured $I-V$. Circles: modeled $I-V$.

Since the new $I-V$ model for planar-doped HEMT's is obtained from the previous model for uniformly doped HEMT's with slight modification of the parasitic conduction region, it is expected that this new model will be as effective and flexible as the original one. The original model has shown good agreement between modeled and measured characteristics for a wide range of HEMT structures [5].

IV. Small-Signal Parameters

HEMT's are generally biased in the normal region without parasitic conduction for optimal low-noise or high-frequency performance. Some of the small-signal parameters in the normal region can be derived analytically with the $I-V$ model. From (A2), which applies to both uniformly doped and planar-doped HEMT's, the intrinsic transconductance before current saturation can be obtained by

$$g_m = \frac{\partial I_D}{\partial V_G} = \frac{Z\mu_2 C_0 V_D}{L(1+V_D/B)}. \tag{11}$$

The transconductance increases with drain voltage before current saturation and is almost inversely proportional to gate length but for the mobility degradation factor $1/(1+V_D/LE_c)$. In practice, the transconductance increases as the gate length is decreased but the dependence is much less than a reciprocal relationship [14]. Note that C_0 is inversely proportional to the thickness of the AlGaAs layer [2]. Therefore high transconductance can be achieved through deep gate recess, which however increases the gate capacitance. The transconductance itself is inadequate for judgment of device performance.

Among other important small-signal parameters is the gate-to-source capacitance, which in the normal region is the capacitance due to the 2DEG only. Thus

$$C_{gs} = \frac{\partial}{\partial V_G} \int_0^L q n_s \, dx. \tag{12}$$

After performing the integration and using (A2), one obtains the gate-to-source capacitance before current saturation as

$$C_{gs} = ZC_0 \left[\frac{ZC_0\mu_2\left(2(V_G - V_{\text{th}})V_D - V_D^2\right)}{I_D} - \frac{V_D}{E_c} \right] \tag{13}$$

$$= ZC_0 L(2 + V_D/LE_c). \tag{14}$$

Therefore high 2DEG density or high C_0 gives high capacitance. And again the gate capacitance cannot be scaled down linearly with decreasing gate length.

In microwave applications, the current gain cutoff frequency (f_T) is frequently used as an indicator of the device speed. If the conventional definition is adopted, i.e.,

$$f_T = \frac{g_m}{2\pi C_{gs}} \tag{15}$$

a simple expression for f_T is obtained by combining (11) and (14). Hence,

$$f_T = \frac{\mu_2 V_D}{2\pi L^2(1 + V_D/B)(2 + V_D/B)}. \tag{16}$$

Since f_T reaches the maximum value when the current just starts to saturate [15], the maximum or optimum f_T is approximately given by

$$f_T(\text{opt}) = \frac{\mu V_{\text{sat}}}{2\pi L^2(1 + V_{\text{sat}}/B)(2 + V_{\text{sat}}/B)} \tag{17}$$

where by (A6),

$$V_{\text{sat}} = \frac{B(V_G - V_{\text{th}})}{B + (V_G - V_{\text{th}})}. \tag{18}$$

The f_T's calculated by using (17) and (18) with the modeling parameters are shown in Fig. 5 along with the measured f_T's [8]. Reasonable agreement is achieved, considering the small gate length and the crude velocity-field relation used in the I–V model [5]. Parasitic conduction occurs when the gate voltage exceeds -0.15 V ($V_{\text{th}}^* = -0.15$ V). Since (17) does not take into account the parasitic conduction, the calculated f_T's at 0 V and -1 V overestimate the device performance. The calculated f_T at -3 V has a large deviation, probably because the large substrate current at the bias point is close to the threshold voltage. It is important to note that the linear charge control relationship of the 2DEG used in the model is inadequate in the subthreshold region as well. To have a better model of the device in the subthreshold region, a more accurate analytic expression of charge control, such as that reported in [16], is helpful. Our model can be further improved for short-gate devices using a more realistic velocity-field relationship which includes the velocity overshoot effect [17]. In general, it is difficult to obtain an analytical expression of device characteristics if fine details of device operation are taken into account.

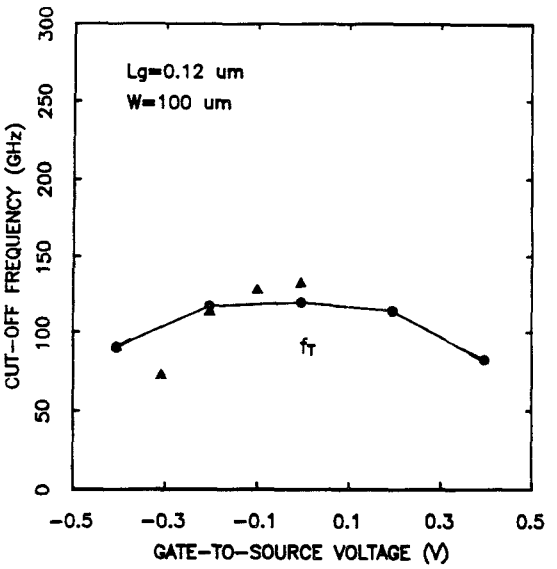

Fig. 5 Measured and calculated f_T of the 0.12×100 μm AlInAs/GaInAs HEMT. Circles: measured f_T from S parameters. Triangles: calculated f_T.

V. Conclusion

We have extended our previous analytic I–V model for uniformly doped HEMT's to be applicable for planar-doped HEMT's. This is the first I–V model derived from physical principles for planar-doped HEMT's. I–V and microwave characteristics can be modeled and predicted using the analytical equations. Because of its many advantages, the planar-doping technique may have potential application in high-volume production of HEMT integrated circuits. The extended model presented in this work provides efficient and accurate device modeling, which is essential for computer simulation of planar-doped HEMT circuits.

Appendix I

The following is a list of the symbols used in the current–voltage model of AlGaAs/GaAs uniformly doped HEMT's:

- μ_1 low field mobility of AlGaAs.
- μ_2 low field mobility of 2DEG.
- E_{c1} saturation electric field of AlGaAs.
- E_{c2} saturation electric field of 2DEG.
- v_s saturation velocity of 2DEG.
- C_0 charge control coefficient.
- V_{th} threshold voltage for 2DEG.
- V_{bi} built-in voltage of the Schottky gate on AlGaAs layer.
- V_p effective pinch-off voltage of AlGaAs layer.
- Z gate width.
- L gate length.
- d thickness of AlGaAs layer.

d_i thickness of undoped AlGaAs layer.
w length of undepleted region in AlGaAs layer.
N_d doping concentration of AlGaAs layer.
n_s sheet charge density of 2DEG.
n_D sheet charge density of doping plane.
n_{s0} equilibrium sheet charge density of 2DEG.
ϵ_2 permittivity of AlGaAs.

Appendix II

The current–voltage model of the uniformly doped HEMT's derived in [5] is reproduced here for reference.

In this model, the HEMT current–voltage characteristics are divided into two regions. When the gate voltage is greater than the threshold voltage of parasitic conduction, the device is working in the suppressed transconductance region; otherwise, the device is in the normal transconductance region, i.e.,

$V_G > V_c$ for suppressed transconductance region

$V_G \leqslant V_c$ for normal transconductance region

where

$$V_c = V_{bi} - \frac{qN_d}{2\epsilon_2}\left(d - d_i - \frac{n_{s0}}{N_d}\right)^2. \tag{A1}$$

A. Normal Transconductance Region

1) Linear Region ($V_D < V_{sat}$): The drain current as a function of gate and drain voltages is

$$I_D = \frac{A\left(V_G - V_{th} - \frac{V_D}{2}\right)V_D}{1 + \frac{V_D}{B}} \tag{A2}$$

where

$$A = \frac{Z\mu_2 C_0}{L} \tag{A3}$$

$$B = LE_{c_2}. \tag{A4}$$

2) Saturation Region ($V_D \geqslant V_{sat}$):

$$I_D = \frac{A\left(V_G - V_{th} - \frac{V_{sat}}{2}\right)V_{sat}}{1 - K_1 + \frac{V_{sat}}{B}} \tag{A5}$$

where

$$V_{sat} = \frac{(1-K_1)B(V_G - V_{th})}{(1-K_1)B + (V_G - V_{th})} \tag{A6}$$

$$K_1 = \frac{-(B+V_D) + \sqrt{(B+V_D)^2 - \left[2CA(V_G - V_{th})^2 - 4B\right]\left[(1 - V_D/B)(V_G - V_{th}) - V_D\right]}}{CA(V_G - V_{th})^2 - 2B}. \tag{A7}$$

B. Suppressed Transconductance Region

1) Linear Region I ($V_D < V_G - V_c$): The 2DEG channel current is

$$I_2 = \frac{A(V_{bi} - V_p - V_{th})V_D}{1 + \frac{V_D}{B}}. \tag{A8}$$

The parasitic conduction current is

$$I_1 = \frac{E}{1 + \frac{V_D}{F}}\left[V_D - \frac{2}{3}\frac{(V_{bi} - V_G + V_D)^{3/2} - (V_{bi} - V_G)^{3/2}}{\sqrt{V_p}}\right] \tag{A9}$$

where

$$E = Z\mu_1 qN_d\left(d - d_i - \frac{n_{s0}}{N_d}\right)\Big/L \tag{A10}$$

$$F = LE_{c_1} \tag{A11}$$

and the total drain current is

$$I_D = I_1 + I_2. \tag{A12}$$

2) Linear Region II ($V_G - V_c \leqslant V_D < V_{sat}$):

$$I_2 = \frac{A\left[\left(V_G - V_{th}\frac{V_D + V_0}{2}\right)(V_D - V_0) + (V_{bi} - V_p - V_{th})V_0\right]}{1 + \frac{V_D}{B}} \tag{A13}$$

$$I_1 = \frac{E\left[V_0 - \frac{2}{3}\left(V_p - \frac{(V_{bi} - V_G)^{3/2}}{\sqrt{V_p}}\right)\right]}{\left[\frac{A(V_{bi} - V_p - V_{th})}{I_2} - \frac{1}{B} + \frac{1}{F}\right]V_0} \tag{A14}$$

where $V_0 = V_G - V_c$.

3) Saturation Region ($V_{sat} \leqslant V_D$):

$$A\left(V_G - V_{th} - \frac{V_{sat}+V_0}{2}\right)(V_{sat}-V_0) + A(V_{bi}-V_p-V_{th})V_0$$

$$I_1 = \frac{E\left[V_0 - \frac{2}{3}\left(V_p - \frac{(V_{bi}-V_G)^{3/2}}{\sqrt{V_p}}\right)\right]}{\left[\frac{A(V_{bi}-V_p-V_{th})}{I_2} - \frac{1}{B} + \frac{1}{F}\right]V_0} \tag{A16}$$

where V_{sat} and K_1 are determined by

$$V_{sat} = \frac{(1-K_1)B(V_G-V_{th})+V_0^2}{(V_G-V_{th})+(1-K_1)B} \tag{A17}$$

$$V_D - V_{sat} = \frac{CAK_1^2\left[(V_G-V_{th})V_{sat} - \frac{V_{sat}^2}{2} - \frac{V_0^2}{2}\right]}{1-K_1+\frac{V_{sat}}{B}} + BK_1. \tag{A18}$$

ACKNOWLEDGMENT

The authors would like to thank Prof. W. H. Ku of UCSD for helpful discussions and Dr. Y. K. Chen of AT&T Bell Labs for technical suggestions.

REFERENCES

[1] D. Delagebeaudeuf and N. T. Linh, "Metal-(n)AlGaAs-GaAs two dimensional electron gas FET," *IEEE Trans. Electron Devices*, vol. ED-29, pp. 955–960, June 1982.

[2] K. Lee, M. S. Shur, T. J. Drummond, and H. Morkoc, "Current–voltage and capacitance-voltage characteristics of modulation-doped field-effect transistors," *IEEE Trans. Electron Devices*, vol. ED-30, pp. 207–212, Mar. 1983.

[3] K. Lee, M. S. Shur, T. J. Drummond, and H. Morkoc, "Electron density of the two dimensional electron gas in modulation doped layers," *J. Appl. Phys.*, vol. 54, pp. 2093–2096, Apr. 1983.

[4] K. Lee, M. S. Shur, T. J. Drummond, and H. Morkoc, "Parasitic MESFET in (Al,Ga)As/GaAs modulation doped FET's and MODFET characteristics," *IEEE Trans. Electron Devices*, vol. ED-31, pp. 29–35, Jan. 1984.

[5] G. W. Wang and W. H. Ku, "An analytical and computer-aided model of the AlGaAs/GaAs high electron mobility transistor," *IEEE Trans. Electron Devices*, vol. ED-33, pp. 657–663, May 1986.

[6] G. W. Wang, I. Ichitsubo, W. H. Ku, Y. K. Chen, and L. F. Eastman, "Large-signal time-domain simulation of HEMT mixers," *IEEE Trans. Microwave Theory Tech.*, vol. 36, pp. 756–759, Apr. 1988.

[7] G. W. Wang, Y. K. Chen, D. C. Radulescu, and L. F. Eastman, "A high-current pseudomorphic AlGaAs/InGaAs double quantum-well MODFET," *IEEE Electron Device Lett.*, vol. 9, pp. 4–6, Jan. 1988.

[8] G. W. Wang, Y. K. Chen, W. J. Schaff, and L. F. Eastman, "A 0.1-μm gate $Al_{.5}In_{.5}As/Ga_{.5}In_{.5}As$ MODFET fabricated on GaAs substrates," *IEEE Trans. Electron Devices*, vol. 35, pp. 818–823, July 1988.

[9] E. F. Schubert, J. E. Cunningham, W. T. Tsang, and G. L. Timp, "Selectively-doped $Al_xGa_{1-x}As/GaAs$ heterostructures with high two-dimensional electron-gas concentration $n_{2DEG} > 1.5 \times 10^{12}$ for field effect transistors," *Appl. Phys. Lett.*, vol. 51, pp. 1170–1172, Oct. 1987.

[10] Y. K. Chen, D. C. Radulescu, P. J. Tasker, G. W. Wang, and L. F. Eastman, "DC and RF characteristics of a planar-doped double heterojunction MODFET," presented at the Int. GaAs and Related Comp. Symp., Las Vegas, NV, Sept. 1986; also in Inst. Phys. Conf. Series, no. 83, 1987.

[11] B. Etienne and V. Thierry-Mieg, "Reduction in the concentration of DX centers in Si-doped GaAlAs using the planar doping technique," *Appl. Phys. Lett.*, vol. 52, pp. 1237–1239, Apr. 1988.

[12] A. Zrenner, H. Reisinger, F. Koch, K. Ploog, and J. C. Maan, "Electronic subbands of a doping layer in GaAs in a parallel magnetic field," *Phys. Rev. B*, vol. 33, no. 8, pp. 5607–5610, Apr. 1986.

[13] J. B. Kuang *et al.*, "Kink effect in submicrometer-gate MBE-grown InAlAs/InGaAs/InAlAs heterojunction MESFET's," *IEEE Electron Device Lett.*, vol. 9, pp. 630–632, Dec. 1988.

[14] L. F. Lester *et al.*, "0.15-μm gate-length double recess pseudomorphic HEMT with F_{max} of 350 GHz," presented at 1988 IEDM, San Francisco, CA, Dec. 1988.

[15] Y. K. Chen *et al.*, "Bias-dependent microwave characteristics of atomic planar-doped AlGaAs/InGaAs/GaAs double heterojunction MODFET's," *IEEE Trans. Microwave Theory Tech.*, vol. MTT-35, pp. 1456–1460, Dec. 1987.

[16] A.-J. Shey and W. H. Ku, "On the charge control of the two dimensional electron gas for analytic modeling of HEMT's," *IEEE Electron Device Lett.*, vol. 9, pp. 624–626, Dec. 1988.

[17] W. T. Masslink, N. Braslau, W. I. Wang, and S. L. Wright, "Electron velocity and negative differential mobility in AlGaAs/GaAs modulation-doped heterostructures," *Appl. Phys. Lett.*, vol. 51, pp. 1533–1535, Nov. 1987.

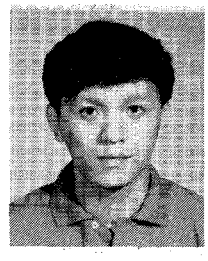

Guan-Wu Wang was born in Taipei, Taiwan, on February 14, 1959. He received the B.S.E.E. degree from National Taiwan University in 1981 and the M.S. and Ph.D. degrees in electrical engineering from Cornell University, Ithaca, NY, in 1985 and 1988, respectively.

In 1988, he joined Ford Microelectronics, Inc., Colorado Springs, CO, to work on HEMT's, HBT's, and other compound semiconductor devices.

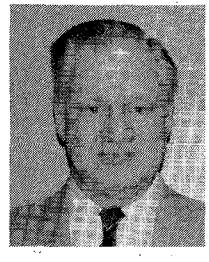

Lester F. Eastman (A'53–M'58–SM'65–F'69) was born in Utica, NY, and obtained the B.S. (1953), M.S. (1955), and Ph.D. (1957) degrees at Cornell University, Ithaca, NY.

He joined the faculty of Electrical Engineering at Cornell in 1957. Since 1965 he has been doing research on compound semiconductor materials, high-speed devices, and circuits, and since 1977 has been active in organizing workshops and conferences on these subjects at Cornell. In 1977 he joined other Cornell faculty members in obtaining funding and founded the National Research and Resource Facility at Cornell (now National Nanofabrication Facility). During the 1978–1979 year he was on leave at MIT's Lincoln Laboratory, and during the 1985–1986 year he was at IBM Watson Research Laboratory. During 1983 he was the IEEE Electron Device Society National Lecturer. He was a member of the U.S. Government Advisory Group on Electron Devices from 1978 to 1988, and serves as a consultant for several industries and Lincoln Laboratory. He has been a member of the National Academy of Engineering since 1986, and was appointed the John L. Given Foundation Professor of Engineering at Cornell in January 1985.